Journal of Computers Vol. 35 No. 2, April 2024, pp. 59-74
doi: 10.53106/199115992024043502004

LDBM-PFR: Local Directional Binary Pattern Mixed Filtering for 2D and 3D Palmprint Fusion Recognition

Sen Lin[1*], Man Li[1], Meng-Zhao Liu[1], Xiang-Ji Fan[2], Peng Shang[1]

[1] School of Automation and Electrical Engineering, Shenyang Ligong University, Shenyang 110159, China
lin_sen6@126.com, {1278584260, 2048768930, 469936432}@qq.com

[2] School of Electronic and Information Engineering, Liaoning Technical University, Huludao 125105, China
1160219445@qq.com

Received 30 July 2023; Revised 9 December 2023; Accepted 3 January 2024

Abstract. Single-dimensional palmprint images are susceptible to interference from noise, lighting, and various factors, leading to information loss and subpar recognition performance. To address the problem, a fusion recognition scheme of 2D and 3D palmprints based on Hybrid Filter Local Orientation Binary Pattern (HFLOBP) is proposed. Firstly, the HFLOBP algorithm is employed to extract 2D features and 3D Shape Index (SI) features respectively to improve the recognition effect. Secondly, Principal Component Analysis (PCA) is utilized to improve the recognition efficiency, to reduce the dimension of 2D features and 3D Surface Type (ST) features of palmprint, to improve the recognition efficiency. Finally, the multi-dimensional palmprint features are fused by Double Weight Threshold Algorithm (DWTA), and classified and recognized by Collaborative Representation (CR). Experimental results conducted on the 3D palmprint database of Hong Kong Polytechnic University reveal that, in comparison with alternative classification methods, the average recognition rate reaches 99.98%, with an average recognition time of 0.64 seconds. The proposed method not only demonstrates a commendable recognition effect but also meets the real-time requirements, underscoring its practical application value.

Keywords: hybrid filter local orientation binary pattern, double-weight threshold, synergistic representation, multi-dimensional palmprint

1 Introduction

To enhance internet capabilities, the need for personal information privacy and security has grown, making the identification of sensitive information increasingly essential. Biometric recognition, an authentication method that analyzes distinctive physiological or behavioral characteristics of the human body, has attracted considerable attention in recent years [1]. Current biometric recognition technologies mainly include fingerprint recognition [2], iris recognition [3], vein recognition [4], face recognition [5], gait recognition [6] etc. Some of the most prominent examples include the forgery of fingerprint identification by using silicone finger sleeves to bypass security checks. While iris and vein recognition boasts high accuracy, acquiring such data is often challenging due to low user acceptance. Conversely, features like face and gait recognition are influenced by age and mood, posing challenges to accurate recognition. Compared with other biometric identification technology, palmprint identification technology [7-8] the advantage of more obvious. Relatively, palmprint recognition suffers from little external interference while containing a wealth of rich information. The simplicity of the collection process also contributes to higher user acceptance compared to more intrusive methods.

So far, palmprint recognition technology has been mainly divided into 2D and 3D palmprint recognition. In 2D palmprint recognition, common methods were categorized into recognition algorithms based on structural features, texture features, subspace features, and deep learning. For example, Xiaojiao Tao et al. [9] extracted EOH-SIFT features of palmprint images for recognition based on fuzzy reasoning rules. This approach had advantages in terms of recognition rate. Zhang et al. [10] used the method of combining the main line of the palmprint and the fusion of texture features, which greatly improved the recognition effect, but the recognition of the three main lines in the palmprint was poor, and it was easy to mismatch. Yuzhen Liu et al. [11] proposed a weighted adaptive multiple unified local binary pattern for feature extraction and utilized two-dimensional principal component analysis to reduce the redundancy of feature vectors. Deep learning has also seen application

* Corresponding Author

within the field of palmprint recognition. Wu et al. [12] extracted palmprint features through the convolution neural network and achieved excellent recognition effects, but the palmprint database is small, making it difficult to train the network and obtain a good parametric model. While the accuracy of 2D palmprint is high, the image acquisition was affected by light changes, random noise, and other factors, resulting in poor image quality. However, using appropriate methods to remove noise and improve the identification accuracy becomes a problem to be solved. Furthermore, the 2D palmprint contains incomplete information and lacks depth information while also being poor in security due to concerns of theft and forgery.

In contrast, 3D palmprint encompasses not only the information found in 2D palmprint but also depth information, rendering reproduction challenging and minimizing external interference. In the field of 3D palmprint recognition, the most popular method currently is the recognition of palmprint curvature features. For instance, literature [13] blocks the surface types of the palmprint and then classifies the collaborative representation. However, the single use of surface type will lead to the loss of detail points and affect the identification accuracy. In literature [14], features were extracted through precise encoding from two primary directions of the palmprint, which enhanced the representation of compact surface types and yielded commendable recognition results. Nevertheless, neglecting the abundant texture information in palmprints could lead to incomplete feature extraction, ultimately affecting the recognition rate. In addition, 3D palmprint features are multi-directional, When the 3D information is mapped to the 2D plane, part of the information will be lost, which cannot guarantee the integrity and accuracy of the directional information of the palmprint.

In summary, to reduce the influence of random noise and other factors on recognition accuracy and solve the problem of information loss in the recognition process, the paper adopts the median filter and wavelet-denoting methods to eliminate the influence of noise. By taking into account the abundant directional information of the palmprint, complementary features are extracted using the main direction and direction confidence of the palmprint to form a local oriented binary pattern (LOBP) and data dimension reduction using principal component analysis. Furthermore, the direct fusion of features of different dimensions will lead to information loss and affect the recognition effect. Therefore, the method of weight allocation is adopted to satisfy the purpose of considering both 2D and 3D features. To improve the timeliness of palmprint recognition, collaborative representation (CR) is selected in the recognition classification algorithm to ensure the recognition speed and achieve high accuracy. Through comparisons with traditional and popular algorithms in palmprint databases, the results show that the proposed algorithm has good recognition performance and meets the actual demands.

The main contributions of this paper are summarized as follows:

1) The double-weight threshold not only takes into account the different dimensions of feature information (different feature dimensions, different features cannot be directly integrated) but also increases the flexibility and adaptability of threshold selection, which helps to enhance the robustness of the algorithm.

2) The features extracted by mixing filters and surface types are high-dimensional features with a lot of redundant information. In this paper, principal component analysis is used to project the feature space to reduce the dimension of features and improve the identification efficiency.

3) The local orientation binary pattern hybrid filtering algorithm to extract the 2D and 3D palmprint features can effectively eliminate the noise, and improve the image quality, and the extracted features complement each other, helping to express the complete palmprint information.

The subsequent sections of this paper are organized as follows. Section 2 provides a review of classic and state-of-the-art methods for palmprint recognition. Section 3 introduces the relevant principles of the feature extraction of the palmprint. Section 4 introduces the feature extraction method, classification matching, and algorithm flow chart proposed in this paper. Section 5 delves into the specifics of the proposed approach, encompassing parameter settings, accuracy, run times, and related details. Finally, section 6 concludes by summarizing the proposed method.

2 Related Works

Currently, research on palmprint recognition can be categorized into two dimensions: 2D palmprint recognition and 3D palmprint recognition. Mainstream 2D palmprint recognition relies primarily on the grayscale features of palmprints to achieve classification and recognition objectives. However, the acquisition process is susceptible to factors such as varying light intensity, environmental noise, and elastic deformation, resulting in poor image quality, incomplete feature extraction, and a significantly diminished recognition effect. Simultaneously, as tech-

nology advances, the risk of counterfeiting 2D palmprints is escalating, underscoring the growing concern about inadequate security. In response, experts and scholars seek a method capable of addressing both incomplete feature challenges in 2D palmprints and enhancing recognition and classification security. This propels 3D palmprint recognition into the spotlight. 3D palmprint images not only encompass the feature information present in 2D palmprint images but also include deeper curvature details, exhibiting robustness against factors like light intensity. This fundamentally aligns with practical application needs, making 3D palmprint recognition more suitable. The identification study of palmprints can be broadly categorized as follows:

(1) Statistical Characteristic Methods: Numerous statistical features exist, with current research primarily concentrating on mean, density, variance, information entropy, and similar mathematical statistical concepts. This method involves classification and identification based on statistical principles. Based on different statistical regions, it can be categorized into global statistics and local statistics. A commonly employed local statistics approach involves partitioning the collected image into uniform blocks and aggregating the palmprint image features through the local characteristics of each small block. For instance, Chen et al. [15] investigated multispectral images using block statistics, enhancing the recognition system's accuracy by combining features from various frequency bands. Minaee et al. [16] applied Gabor transformation to extract meaningful information features in the spatial domain, achieving a commendable recognition effect based on block statistics. However, a standalone statistical method often proves insufficient, necessitating the integration of other characteristic methods to achieve optimal results.

(2) Method of the subspace: The subspace method is a recognition method from complex to simple. The specific principle is to transform the high-dimensional feature information into the low-dimensional representation feature through a series of spatial transformations, and then complete the recognition and matching, namely dimension reduction operation. Zhou et al. [17] utilized the Gabor filter to extract feature information and then reduced the dimensionality of the multidimensional features through various methods, ensuring that the recognition effect could meet the actual requirements. Yao et al. [18] considered the weight matrix of the Locality Preserving Projection (LPP) from the perspective of supervision, and employed the norm to constrain the loss function and the regression matrix, and the classification effect was satisfactory. However, the method of subspace dimensionality reduction needs to select an appropriate threshold and eliminate the threshold cases that do not meet the threshold, which is easy to cause the problem of information loss.

(3) Texture Feature Method: The approach of classifying and recognizing palmprints by extracting local or global texture features is known as the texture feature method. Mokni et al. [19] employed the Gabor filter and the Gray-Level Co-occurrence Matrix (GLCM) to extract palmprint texture information, utilizing the Generalized Discriminant Analysis (GDA) method to reduce feature vector redundancy and achieve optimal recognition rates. Latha et al. [20] modified the Gabor filter type to extract texture features, demonstrating notably effective classification recognition in experimental results. Zhang et al. [21] focused on extracting features such as scale transformation invariance in palmprints, employing the weighted sparse representation method for recognition, which greatly improved the recognition accuracy. However, it is worth noting that the expressed texture features may be incomplete, leading to potential gaps in feature extraction.

(4) Deep Learning Methods: The integration of deep learning with palmprint recognition not only facilitates the adjustment of filter parameters but also leverages the benefits of big data statistics to extract more comprehensive palmprint features, addressing certain limitations of traditional algorithms. Sun et al. [22] employed a CNN-F convolutional network to progressively apply convolution to features obtained layer by layer, resulting in successful palmprint recognition. Shuping et al. [23] extracted palmprint features using a Deep Discriminative Representation (DDR) network, employing a classifier based on collaborative representation for recognition and classification. Hailun et al. [24] utilized various convolutional networks for matching and deep learning yielded significant effects, it's noteworthy that, owing to the limited number of palmprint samples, the deep learning network may encounter overfitting during the training process, impacting the recognition rate.

The aforementioned research methods often focus on isolating individual feature information in images, potentially leading to the omission of essential feature details. Therefore, we propose a 2D and 3D palmprint fusion recognition scheme based on the Hybrid Filter Local Directional Binary Pattern (HFLOBP). Initially, the HFLOBP algorithm is employed to extract both 2D and 3D palmprint features, enhancing the completeness of the extracted features by complementing each other. Subsequently, the Double Weight Threshold Algorithm (DWTA) is utilized to fuse these features. Finally, during the matching stage, principal component analysis and collaborative representation are employed to reduce dimensionality and classify the data, thereby effectively enhancing the performance of palmprint recognition.

3 Principle Introduction

3.1 3D Curvature Feature Extraction

The 3D palmprint is abundant in rich spatial and directional information, and the curvature features, mainly consisting of the Mean Curvature (MC) and Gaussian Curvature (GC), can overcome the adverse effects caused by rotational translation and make up for the deficiency of 2D palmprint recognition. The combination of the two curvatures fully represents the depth information of a 3D palmprint. For any palmprint, the Gaussian curvature and the mean curvature can be expressed as follows:

$$H_{\mathrm{GC}} = \frac{H_{xx}H_{yy} - H_{xy}^2}{(1 + H_x^2 + H_y^2)^2} . \tag{1}$$

$$H_{\mathrm{MC}} = \frac{(1 + H_x^2)H_{yy} + (1 + H_y^2)H_{xx} - 2H_xH_yH_{xy}}{2(1 + H_x^2 + H_y^2)^{3/2}} . \tag{2}$$

Where: H_x, H_y is $H(x, y)$ the first partial derivative, H_{xx}, H_{yy} is $H(x, y)$ the second partial derivative, H_{xy} is $H(x, y)$ the mixed partial derivative.

3.2 Shape Index Extraction

Shape Index (SI) [25] can describe the local texture of 3D palmprint in detail, with scale invariance and stability. For any point on the surface S defined as point a, all curves after point a are expressed as β_i, the curvature of the curve β_i at point a is defined as δ_i, the maximum and minimum of curvature δ_i are set as δ_i and δ_2, respectively, and consider both as the main curvature at point a. The main curvature at point a can be obtained through the Gaussian curvature and the mean curvature, and the formula is calculated as follows:

$$\delta_1 = MC + \sqrt{MC^2 - GC} . \tag{3}$$

$$\delta_2 = MC - \sqrt{MC^2 - GC} . \tag{4}$$

According to the main curvature δ_1 and δ_2, the shape index S_{SI} of the palmprint can be further obtained, as shown in the following equation (5):

$$S_{SI} = \frac{1}{2} - \frac{1}{\pi}\arctan\frac{\delta_1 + \delta_2}{\delta_1 - \delta_2} . \tag{5}$$

Fig. 1 illustrates the shape index diagram of the 3D palmprint, revealing the distinctive line characteristics of the palmprint. Fig. 1: a) depicts the 3D palmprint acquisition image, while b) represents the image after shape index (SI) extraction.

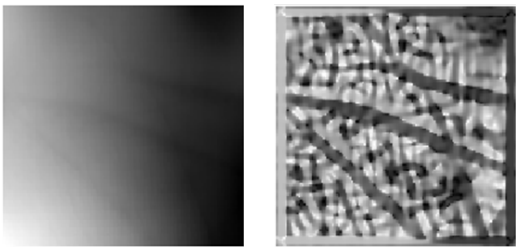

(a) 3D palmprint image (b) SI features were extracted

Fig. 1. 3D palmprint mapping (SI)

3.3 3D Surface Type Extraction

To specifically describe the depth information of the 3D palmprint, the surface is separated into 9 categories based on the curvature characteristics, referred to as the Surface Type (ST) [25], and expressed as H_{ST}. The surface types are extremely discriminatory and can effectively inhibit the misalignment of palm lines. The type is defined by comparing the size relationship of H_{MC}(H_{GC})with the zero value and indicates that the special surface types of $H_{GC} > 0$ and $H_{MC} = 0$, called the minimum surface, do not exist in practical application, but are utilized to ensure the integrity of the data. Any point in the 3D palmprint can be divided into one of the nine surface types, as shown in Table 1:

Table 1. Surface type

	$H_{GC}>0$	$H_{GC}=0$	$H_{GC}<0$
$H_{MC}<0$	Peak ($H_{ST}=1$)	Ridge ($H_{ST}=2$)	Saddle ridge ($H_{ST}=3$)
$H_{MC}=0$	None ($H_{ST}=4$)	Flat ($H_{ST}=5$)	Minimal surface ($H_{ST}=6$)
$H_{MC}>0$	Pit ($H_{ST}=7$)	Vally ($H_{ST}=8$)	Saddle valley ($H_{ST}=9$)

Through the above steps, the ST image can be obtained from the ROI image of 3D palmprint, and the image can be cascaded and block statistical processing, which can effectively reduce the registration error in the recognition process, to further enhance the depth characteristics of palmprint. As shown in Fig 2: a) 3D palmprint image, b) ST image.

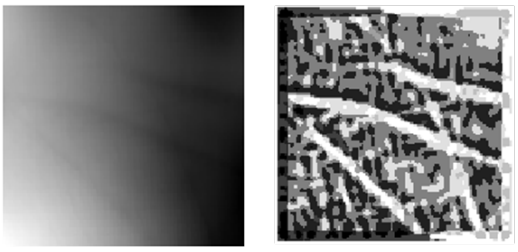

(a) 3D palmprint image (b) ST features were extracted

Fig. 2. 3D palmprint mapping (ST)

For a more intuitive understanding, Fig. 3 gives the basic type of ST, as a supplementary illustration to Table 1, length width, and height represent the *x*, *y* and *z* axis respectively.

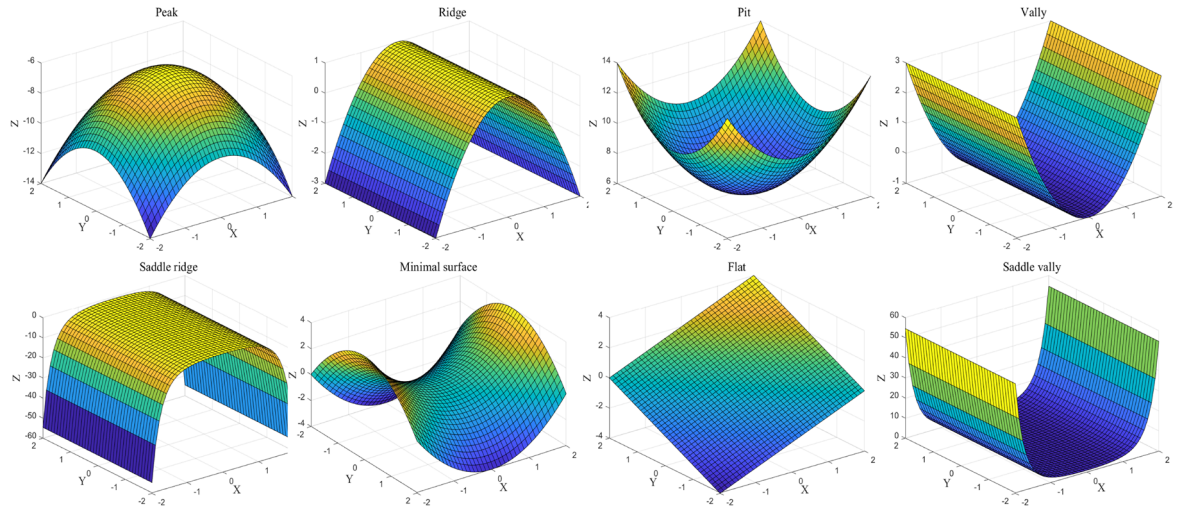

Fig. 3. Eight basic surface types

The ST feature derived from the shape index graph exhibits a dimension inconsistency with the HFLOBP feature, making direct fusion challenging. In this study, the two features are amalgamated by establishing a weight threshold, thereby creating a comprehensive feature vector for the 3D palmprint.

4 Proposed Method

4.1 Hybrid Filtering Algorithm

In the process of collection, the palmprint image is easily affected by the equipment, lighting, and other factors, leading to the reduction of the image quality and poor recognition effect. Therefore, to eliminate noise and sharpen the acquired image, the processes of the hybrid filter combined with the Median Filter [26] and the Wavelet Denoting [27] method are utilized, the pseudocode for the hybrid filter is presented in Table 2:

(1) Median Filtering

The median filter is a widely employed image filtering algorithm designed to eliminate noise from images. This method diminishes burst noise in the image by substituting the gray value of each pixel with the median value within its vicinity.

(2) Wavelet Denoting

Wavelet transform [27] proves to be an effective means of mitigating the impact of noise on an image, ensuring the preservation of essential feature information. Through wavelet transformation, the original image is converted into wavelet coefficients, which can be quantized using a threshold value. Those wavelet coefficients exceeding the threshold signify the co-variation of signal and noise and are consequently reduced. This threshold-based processing proves effective in noise elimination while preserving image details. By inverting the wavelet coefficients after processing, the wavelet coefficients can be synthesized into an image, that is, image reconstruction. The image processed in this way can effectively remove the noise while retaining the details and feature information of the original image to achieve the effect of image polishing.

Table 2. Hybrid filter pseudocode

Algorithm.
Input: input image I **Output:** output image H_SI
1. Procedure process: CreateFeature (I) % Obtains the features of the image I
2. [k_1, k_2] = qulvcurvature (I); % Curvature characteristic
3. SI = 0.5- (atan2 (k_1 + k_2, k_1-k_2)) / pi; % The SI image was acquired through the tangent function
4. M_SI = medfilt2 (SI, [3,3]); % Median filter
5. [C] =wavedec2 (M_SI, 2, 'sym 5'); % Wavedec2 wavelet decomposition
6. [T, $sort$, $keepapp$] = ddencmp('den', 'wv', M_SI); % Ddencmp Used for noise reduction
7. If | C_i |> T Y_i = sgn (C_i) (|C_i | - δ) % 7-8 is the coefficient contraction
8. else Y_i=0;
9. [H_SI]=wdencmp('gbl',Y_i,'sym5',2,sort,keepapp); % Wavelet reconstruction
End process

4.2 2D Palmprint Feature Extraction

As 2D palmprint focuses on the points, lines, and veins of the palmprint surface, and is susceptible to the influence of elastic deformation, random noise, and other factors in the recognition process [28]. Therefore, the paper proposes the HFLOBP algorithm to extract 2D palmprint features. The hybrid filter in the algorithm not only inhibits the noise but also protects the edge information of the image. Fig. 4 shows the 2D palmprint acquisition images and the filtered processed images.

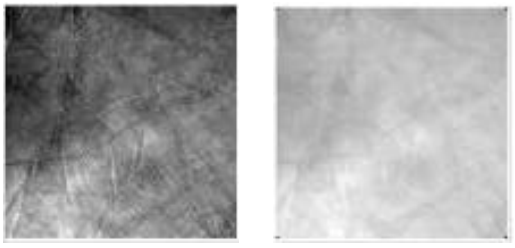

(a) 2D palmprint image (b) Images after filtering

Fig. 4. 2D palmprint and mixed filter image

To further improve the recognition accuracy, the filtered 2D palmprint images were segmented and cascaded to obtain the HFLOBP feature descriptors of 2D palmprint, However, the dimensions of the features are large, resulting in low identification efficiency. Therefore, principal component analysis (PCA) was used to reduce the characteristics. The feature values and feature vectors are obtained by singular value decomposition of the image after feature extraction. The descending arrangement of eigenvalues can effectively eliminate the influence of smaller eigenvalues on recognition accuracy. In addition, PCA can effectively reduce dimension and retain feature vectors with large eigenvalues, thus reducing data dimensions: 32640*n to 4000*n (where n is the number of training samples), thus effectively improving recognition efficiency.

4.3 Local Directional Binary Pattern

The palmprint image contains abundant directional features. After mixed filtering, the Gabor filter is used to extract directional features. Specific steps are described as follows:

Step 1: This paper extracts the directional features from six different directions, namely: $\theta_i = \frac{i\pi}{6}(i = 0,1...,5)$. In the feature extraction of palmprint direction, a convolution operation is carried out between the real part of Gabor and the palmprint image:

$$c_{\mathrm{j}}(x,y) = G_{\mathrm{j}}^{\mathrm{r}} \otimes \left(255 - I(x,y)\right) \ . \tag{6}$$

Where: $c_j(x, y)$ the convolution result, G_j^r the real part of the Gabor filter, $I(x, y)$ represents the input image.

Therefore, the main direction of the palmprint lines is as follows:

$$o(x,y) = \arg\max_{j} c_{\mathrm{j}}(x,y) \ . \tag{7}$$

Step 2: Obtain the orientation confidence of the palmprint through the main direction of the palmprint as follows:

$$c_{\mathrm{o}}(x,y) = c_{o(x,y)}(x,y) = arg\max_{c} c_{\mathrm{j}}(x,y) \ . \tag{8}$$

Where: $c_{o(x, y)}(x, y)$ is the maximum value of the convolution response.

Step 3: According to the principal direction and orientation confidence of the palmprint, the following formula is used to obtain the orientation binary pattern (OBP) and confidence binary pattern (CBP) of the palmprint.

$$V_{\mathrm{OBP}} = \sum_{i=1}^{8} e(o_i, o_c)2^i \ . \tag{9}$$

$$V_{\mathrm{CBP}} = \sum_{i=1}^{8} s(c_{o,i} - c_{o,c})2^i \ . \tag{10}$$

Where O_i and O_c represent the main direction of the neighboring pixel and the central pixel respectively, $C_{o, j}$ and $C_{o, c}$ indicate the orientation confidence of the neighboring pixel and the central pixel respectively.

Step 4: The OBP and CBP features of the palmprint image are complementary, and the two combine to form a local orientation binary pattern (LOBP).

Combining the hybrid filtering algorithm with the local directional binary algorithm, called HFLOBP feature descriptors. The algorithm can effectively eliminate the influence of noise and enhance the correlation of the surrounding pixels. The accuracy of direction coding can be improved by jointly representing the direction information.

4.4 Double-Weight Threshold Algorithm

Because the surface type and shape index characteristic dimensions of 3D palmprint are not consistent, the Dual Weight Threshold Algorithm (DWTA) [29-30] is used for the combination. As shown in the following formula:

$$V = \lambda_1 \times T + (1 - \lambda_1) \times I \quad \lambda_1 \in (0,1) \ . \tag{11}$$

Where V, T, and I represent the combined 3D features, surface type features, and shape index features respectively, while the parameter λ_1 is the weight threshold operator.

Similarly, when combining 3D and 2D palmprint features, the weight operator λ_2 is set by the following equation.

$$M = \lambda_2 \times V + (1 - \lambda_2) \times D \quad \lambda_2 \in (0,1) \ . \tag{12}$$

Where: M, V, and D represent the combined palmprint features, 3D features, and 2D features respectively, and the parameter λ_2 is the weight threshold operator.

The algorithm based on the double-weight threshold not only considers the different feature information dimensions but also increases the flexibility and adaptability of the threshold selection, which helps to enhance the robustness of the algorithm.

4.5 Collaborative Classification Method

The classification idea of Collaborative Representation [9] (CR) uses the l_1 norm to replace the l_2 norm of sparse classification representation. Sparse classification based on l_1 norm requires a large amount of computation and cannot reflect the problem of collaborative classification. However, collaborative classification based on norm, otherwise known as Classification Based on Collaborative Representation and Rule Least Squares (CRC_RLS), solves this problem.

The steps of CRC_RLS are as follows:

Step 1: Class N palmprint training set is represented by $X = [X_1, X_2, ..., X_K]$, and the training sample of the class i is defined as $X_i = [v_{i,1}, v_{i,2}, ..., v_{i,j},] \in \mathrm{R}^{m \times n_i} \quad (j = 1, ..., n_i)$.

Where, v_{ij} represents the feature vector corresponding to the j sample of the class palmprint, and n is the dimension of the feature vector.

Step 2: If $y \in R^m$ represents the feature vector of a test sample, use the feature vector of the training sample set to linearly represent y, namely: $y \approx A\chi$, $\chi = [\chi_1; \chi_2; \chi_3; ...; \chi_k]$, where χ_i is the coding coefficient vector of class i.

Step 3: If $y = X\chi$ is established, then the feature vector y of the test sample belongs to the class palmprint. When test samples are represented jointly based on all training samples, to reduce computational complexity, y is used to replace the problem of solving l_1 norm in sparse representation idea with the problem of solving the regular least square method. The calculation formula is as follows:

$$\left(\hat{\chi}\right) = \arg\min_{\chi} \{ \| y - A\chi \|_2^2 + \lambda \| \chi \|_2^2 \} \ . \tag{13}$$

Step4: Compared with sparse representation, the formula used in step 3 is less complex than directly solving the l_1 norm optimal solution problem, and the calculation formula is as follows:

$$\hat{\chi} \Rightarrow (X^T X + \lambda I)^{-1} X^T y = Py \quad . \tag{14}$$

In the process of identifying the test sample y, the coefficient vector can be directly calculated by projecting y onto P, and then Py can be obtained. This method can reduce the computational complexity and thus shorten the calculation time.

4.6 Algorithm Scheme

The process of HFLOBP feature descriptors of multidimensional palmprint images is shown in Fig. 5. The specific steps are as follows:

Step 1: The ST and SI images are obtained according to the curvature characteristics of the 3D palmprint image;

Step 2: Mixed filtering of 3D SI image and 2D palmprint image, extracting OBP and CBP feature histograms, to obtain HFLOBP features;

Step 3: Use the PCA method to reduce the ST features of 3D palmprint and HFLOBP features of 2D palmprint;

Step 4: Realize the combination of 2D and 3D palmprint images through DWTA method;

Step 5: The CRC_RLS method is given to achieve the matching classification of the images.

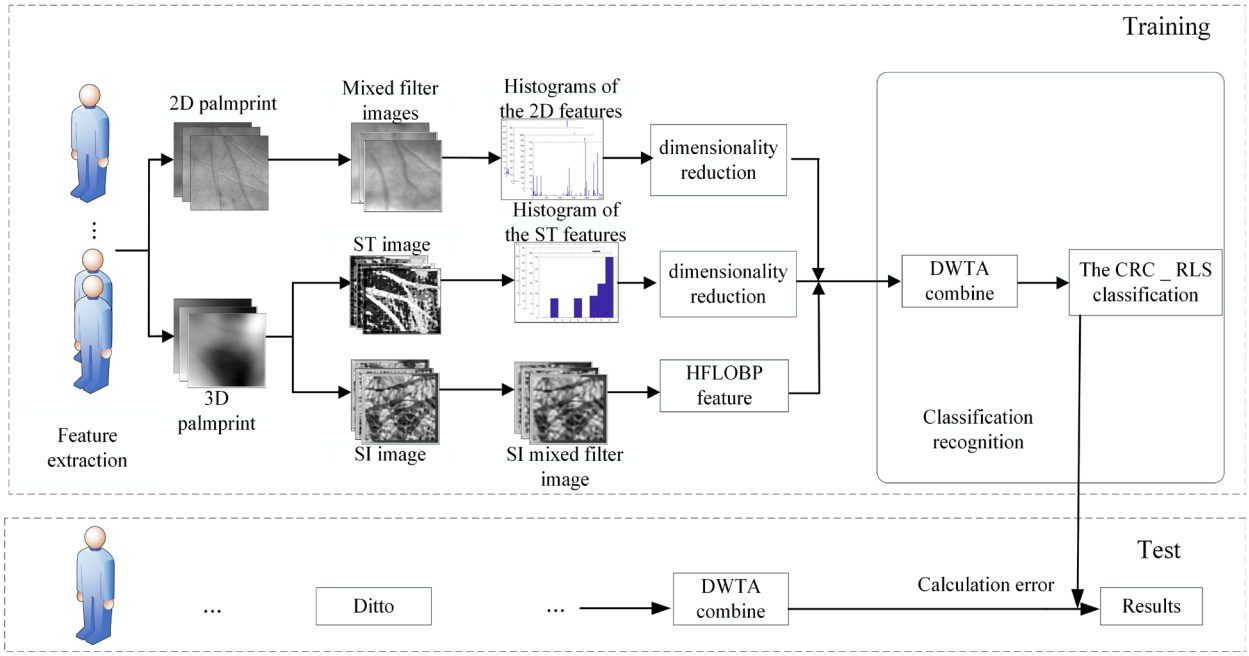

Fig. 5. Flow chart of the algorithm

5 Experimental Results and Analysis

5.1 Description of the Dataset and the Experimental Environment

The experiment was conducted on the Hong Kong Polytechnic University Open Palmprint Database, which contains 8,000 3D palmprint samples and corresponding 2D palmprint samples. The left and right palmprint information of 200 volunteers was collected, with ten pieces of information collected each time, and the collection interval was 30 days. During the experiment, the images collected from the same palm can be regarded as the same class, while the images collected from different palms are different classes. The database contains 400 classes, and each class contains 20 samples. The hardware specification of the experimental platform is a Windows 10 system, the central processor is AMD Ryzen3 4300U, the main frequency is 2.7GHz, and the running memory is 8GB.

5.2 Noise Elimination Experiment

Palmprint images typically exhibit salt and pepper noise as well as Gaussian noise, making it challenging to visually discern the transformations within the image from a subjective standpoint. In this section, we intentionally introduce a significant amount of mixed noise (comprising salt and pepper noise and Gaussian noise) into the original image to simulate the impact of a noisy image. The results of the noise elimination experiment are presented in Fig. 6:

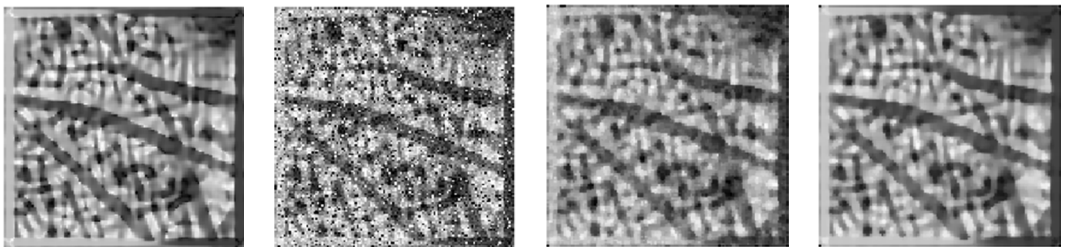

(a) Original drawing (b) Mixed filter plot (c) Filtered image (d) Original image filtering

Fig. 6. Image without noise elimination

As evident in Fig. 6(b), a substantial quantity of noise in the image significantly compromises the overall image quality, thereby detrimentally impacting the recognition result. Fig. 6(c) illustrates the results after employing the median filter and wavelet denoising for noise elimination. The observed blurriness is attributed to the substantial noise added to the original map, resulting in excessive smoothing after applying the filtering techniques. In Fig. 6(d), the filtered image reveals a noticeable improvement, showcasing a smoother appearance.

To objectively assess the influence of filtering on recognition accuracy, N (where N = 2, 3, 4) images were randomly chosen as the training set, while the remaining images constituted the test set. This process was repeated in ten experiments, and the average value of each result is documented in Fig. 7:

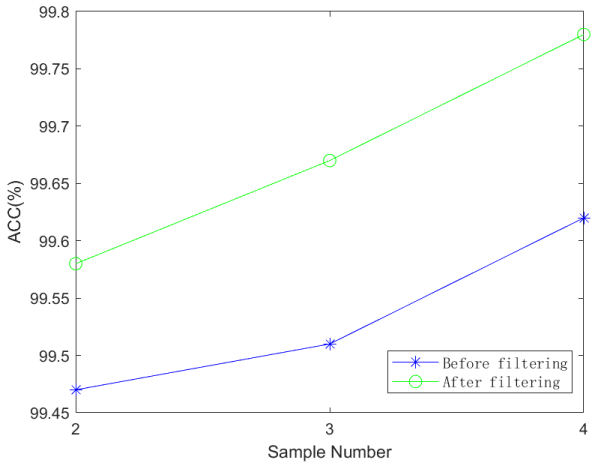

Fig. 7. Comparison of recognition accuracy before and after noise elimination

As depicted in Fig. 7, there was a noticeable change in recognition accuracy before and after filtering. This indicated that the image filtering operations implemented as part of the preprocessing in this study effectively eliminated noise and diminished interference, contributing to enhanced recognition accuracy.

5.3 Block Statistical Experiment

During the palmprint recognition process, features were extracted using block statistics, effectively enhancing local texture information. The number of blocks had a significant impact on the recognition effect and efficiency. By setting different block methods for comparison experiments, the samples collected in the first and second stages were taken as the training set and the test set, respectively. The experiment was repeated 10 times and the results were recorded. Table 3 records the feature extraction time, classification identification time, and identification rate under different block methods.

Table 3. Block statistical table

Blocked mode	2D extraction time/s	3D extraction time/s	Classification identification time/s	Accuracy/%
2×2	0.1316	**0.1655**	0.2649	90.87
3×3	0.1071	0.1701	0.2428	93.64
4×4	0.0969	0.1779	0.2410	94.73
5×5	0.0940	0.1796	0.2355	97.12
6×6	**0.0871**	0.1814	0.2218	98.20
7×7	0.0890	0.1825	**0.2144**	99.07
8×8	0.0915	0.1834	0.2210	**99.85**
9×9	0.0943	0.1886	0.2457	98.80
10×10	0.0953	0.2058	0.2601	96.15

It can be found from Table 3 that 3D extraction time increases in response to an increase in the number of blocks, while the 2D feature extraction time and classification identification time show a trend of decreasing first and then rising.

The alternating trend of the extraction and identification time was indicative that a gradual increase in the number of palmprint marks was beneficial to shorten the recognition process, however, with the increase in the number of blocks, the palmprint information became difficult to extract in the local area. On the other hand, 3D palmprint feature extraction could be divided into two parts: surface type feature and shape index feature. The shape index feature itself has a small dimension, and the increase in block number has little influence on it. With the increase in the number of blocks, the feature dimension of the surface type increases, and the extraction time of 3D palmprint features increases after the combination of the two. The classification identification time depends on the extracted palmprint features. As could be seen from the data, its change trend was generally on the rise, indicating that the increase in the number of blocks at the beginning was indeed conducive to the recognition process, but as the critical point approached, the overall recognition efficiency began to decline.

Affected by the three factors, the recognition rate presented a changing trend of first rising and then falling. When the 8×8 block method was adopted, the recognition rate reached the maximum of 99.85%. Based on the above factors, the subsequent experiments were carried out based on the 8×8 block method on the premise of giving priority to the recognition effect.

5.4 Ablation Experiments

To prove the effectiveness of the algorithm binding in this paper, the following experiments were performed under the same conditions to compare the recognition rates of the single-feature algorithm and the multi-feature binding algorithm respectively. The number of training samples for each palmprint line N was increased from 3 to 10 and the test samples were randomly selected and run 10 times to obtain the average identification rate corresponding to different numbers of samples.

As evidenced in Fig. 8, the recognition accuracy of extracting a single feature is low, likely caused by the fact that a single feature contains less information and is affected by noise (only hybrid filtering processing is carried out for the fusion scheme in this paper). The curve of the palmprint recognition scheme in this paper was much higher than that of other schemes, and relatively stable. Because this paper extracted feature information from multiple angles, the PCA algorithm was used to discard the feature vector corresponding to the smaller eigenvalue, reducing the interference, and thus improving the recognition accuracy. Furthermore, the overall recognition scheme demonstrates high precision, better reflecting the effectiveness of the proposed algorithm and its practical value.

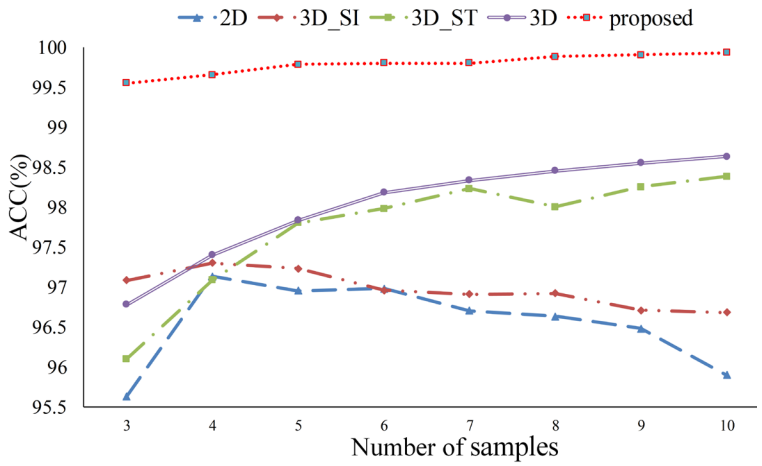

Fig. 8. Fusion experiment

5.5 The Weight Threshold Selection Experiment

In this paper, λ_1 and λ_2 are set as the threshold operators of the double-weight algorithm in consideration of the different amounts of information contained by different features in the process of feature combination. These operators were set in the range of 0 to 1. In this section, the influence of the operator on the recognition effect was explored experimentally, and the operator value that maximizes feature expression is found. The 400 types of samples collected in the first stage were taken as the training set, and the 400 types of samples collected in the second stage were taken as the test set. With 0.1 as the starting point and 0.2 as the step length, the experiment was repeated ten times. Fig. 9 shows the 3D image of the change of the recognition rate double weight threshold operator.

The experimental results indicate that when λ_1 and λ_2 are set to 0.3 and 0.1, respectively, the recognition effect reaches a high of 99.98%. As a result, these values will be implemented in the subsequent experiments as the best weight threshold operator.

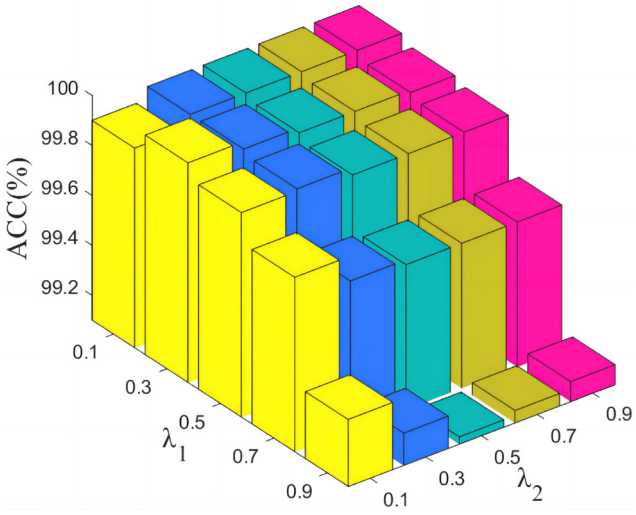

Fig. 9. Two-weight threshold operator change image

5.6 Palmprint Recognition Experiment

Palmprint recognition determines its label category by comparing the distance between the test set and the training set. Several palm lines were randomly selected to form the training set, with the remaining Palmprint lines making up the test set. Different sample numbers were run 10 times to calculate the mean value. The proposed method was compared with other recognition methods such as the 2D Gabor method, Contourlet fusion, wavelet fusion [31], LOBP_CR [32], Daisy+SIFT [33], and AlexNet_ST [34]. The experimental results are shown in Table 4. When the palmprint images with different training samples were selected, the total average value of the proposed method increased by 2.59%, 1.67%, 0.81%, and 0.63%, respectively, compared with other methods.

Table 4. Quantitative comparison of recognition rate

N	2DGabor	Contourlet-Fusion	wavelet fusion	Daisy+SIFT	AlexNet_ST	LOBP_CR	Propose
1	94.10%	94.10%	93.39%	98.95%	91.37%	95.53%	**98.22%**
2	96.95%	98.20%	98.02%	99.42%	95.83%	99.04%	**99.58%**
3	97.11%	99.01%	98.95%	99.67%	99.05%	99.32%	**99.67%**
4	97.62%	99.50%	99.13%	99.72%	99.40%	99.48%	**99.78%**

As observed in Table 4, the identification accuracy in this study has shown significant improvement. In comparison to LOBP_CR, our algorithm not only captures 3D information but also acquires feature data from the 2D palmprint, creating a complementary relationship. In contrast to alternative algorithms, the abundance of features extracted in this study enables a more precise description of palmprint characteristics. Furthermore, deep learning algorithms, lacking a comprehensive palmprint image database for adequate training, exhibit lower recognition accuracy than our proposed algorithm.

5.7 CRC _ RLC Classification Performance Experiment

To verify the performance of CRC_RLS in the identification method, the classification method is compared with the more popular methods, such as SpaRSA, DALM, Homotopy, denoted as CR_L_1_SpaRSA, CR_L_1_DALM, CR_L_1_Homotopy, respectively. The 400 samples collected in the first stage ($N = 10$) were used as the training set, and the 400 samples collected in the second stage were used as the test set. Under the same equipment environment, the three comparison methods and our novel method were run 10 times respectively, and the mean value of the identification rate and identification time (including training and classification identification) were calculated in Table 5.

Table 5. Comparison of methods based on collaborative representation

Classification method	Accuracy/%	Recognition time/s
CR_L1_SpaRSA	99.14	47.22
CR_L1_DALM	99.32	10.47
CR_L1_Homotopy	99.57	0.98
Proposed method	99.98	0.64

Referring to Table 5, our algorithm showcases an average recognition time of 0.64 seconds, marking a significant improvement of 46.58 seconds, 9.83 seconds, and 0.34 seconds when directly compared to other methods. Additionally, a recognition rate enhancement of 0.84%, 0.66%, and 0.41% is observed when compared with alternative recognition methods. The classification method employed in this study proved notably more efficient than others, utilizing the l_2 norm instead of the l_1 norm, thereby resolving the issue of high computational complexity associated with the sparse representation of the l_1 norm. Consequently, the classification identification method adopted in this paper exhibits superior performance while also demonstrating practical value in real-world applications.

6 Conclusions

Aiming at the problem of poor recognition rate caused by incomplete expression of feature information in 2D and 3D palmprint images, the fusion recognition of 2D and 3D palmprint based on local direction binary mode hybrid filtering is proposed. The novel method not only demonstrates a substantial improvement in feature extraction but also satisfies the recognition efficiency in practical application. Initially, the HFLOBP features of 2D palmprint images were extracted, and the dimensionality of the features was reduced by the PCA method to avoid the problem of an excessive feature processing time caused by impractical dimension sizes. Then, the surface type feature and shape index map of the 3D palmprint image were obtained according to the curvature, and the HFLOBP feature based on the shape index map was extracted while the surface type feature dimension was reduced. Secondly, the DWTA algorithm was employed to combine the surface type features, HFLOBP features based on shape index map, and 2D palmprint. The process specifically addresses the issue of information loss resulting from different dimensions, ensuring a more comprehensive effect. Finally, the CRC_RLS classification method is used for recognition, which effectively reduces computational burden while preventing data sparsity. Through experimentation on the public palmprint database from Hong Kong Polytechnic University, the results demonstrate that the average recognition rate and identification times can reach 99.98% and 0.64s, respectively, under optimal conditions.

Owing to constraints within the palmprint database, the recognition performance in deep learning is not yet optimal. To overcome this limitation, initiatives will be undertaken to expand the relevant databases. Furthermore, with the advent of multimodal recognition, there is a consideration of integrating palmprint recognition with other modes to enhance overall recognition accuracy.

Additionally, when factoring unaccountable delays in real-world application of the recognition time, any future work will prioritize the need to improve recognition time and efficiency as a core focus.

7 Acknowledgement

This research was supported by the National Key R&D Program of China funded by the Ministry of Science and Technology of the People's Republic of China (No. 2018YFB1403303); The Educational Departments of Liaoning Province Basic Research Project for Higher Education Institutions (LJKMZ20220615)

References

[1] S. Khan, S. Parkinson, L Grant, N. Liu, S. Mcquire, Biometric systems utilizing health data from wearable devices: applications and future challenges in computer security, ACM Computing Surveys (CSUR) 53(4)(2021) 1-29.

[2] J. Priesnitz, C. Rathgeb, N. Buchmann, C. Busch, M. Margraf, An overview of touchless 2D fingerprint recognition, EURASIP Journal on Image and Video Processing 2021(1)(2021) 1-28.

[3] A. Boyd, S. Yadav, T. Swearingen, A. Kuehlkamp, M. Trokielewicz, E. Benjamin, P. Maciejewicz, D. Chute, A. Ross, P. Flynn, K. Bowyer, A. Czajka, Post-mortem iris recognition—a survey and assessment of the state of the art, IEEE Access 8(2020) 136570-136593.

[4] Z.-Y. Tao, M. Wang, X.-R Zhou, J. Li, S. Lin, Ffv-Mbc: A Novel Fused Finger-Vein Recognition Method Based on Monogenic Binary Coding, Journal of Computers 34(1)(2022) 13-27.

[5] I. Adjabi, A. Ouahabi, A. Benzaoui, A. Taleb-Ahmed, Past, present, and future of face recognition: A review, Electronics 9(8)(2020) 1188.

[6] J.-W. Gao, C. Ma, J. Yao, S.-H. Wang, Research on intelligent recognition algorithm of human gait detection based on machine learning, Journal of Electronic Measurement and Instrumentation 35(3)(2021) 49-55.

[7] Y. Xu, L.-K. Fei, J. Wen, D. Zhang, Discriminative and robust competitive code for palmprint recognition, IEEE Transactions on Systems, Man, and Cybernetics: Systems 48(2)(2018) 232-241.

[8] L.-K. Fei, G.-M. Lu, W. Jia, S.H. Teng, D. Zhang, Feature extraction methods for palmprint recognition: A survey and evaluation, IEEE Transactions on Systems, Man, and Cybernetics: Systems 49(2)(2019) 346-363.

[9] X.-J. Tao, J. Lu, Palmprint recognition based on integrated filtering EOH-SIFT features and fuzzy reasoning, Modern Electronics Technique 43(4)(2020) 73-77.

[10] Z.-M. Zhang, Recognition method for the fusion of palmprint main line and texture features, Electronic Technology & Software Engineering 171(1)(2020) 122-126.

[11] Y.-Z. Liu, X.-L. Wang, S. Lin, Palmprint recognition method by combining weighted adaptive MULBP and 2DPCA, Journal of Electronic Measurement and Instrumentation 35(1)(2021) 142-150.

[12] T. Wu, L. Leng, M.-K. Khan, F.A. Khan, Palmprint-palmvein fusion recognition based on deep hashing network, IEEE Access 9(2021) 135816-135827.
[13] L. Zhang, Y. Shen, H.-Y. Li, J.-W. Lu, 3D palmprint identification using block-wise features and collaborative representation, IEEE Transactions on Pattern Analysis and Machine Intelligence 37(8)(2015) 1730-1736.
[14] X. Wang, S.-Y. Gai, F.-P. Da, Fusion of geometric and orientation information for 3d palmprint recognition, Journal of Graphics 41(3)(2020) 390-398.
[15] H. Chen, An efficient palmprint recognition method based on block dominat orientation code, Optik-International Journal for Light and Electron Optics 126(21)(2015) 2869-2875.
[16] S. Minaee, A.-A. Abdolrashidi, Highly accurate palmprint recognition using statistical and wavelet features, in: Proc. IEEE Signal Processing and Signal Processing Education Workshop, 2015.
[17] P. Yu, H. Li, H. Zhou, D. Xu, Palmprint recognition based on subclass discriminant analysis, in: W.E. Wong, T. Zhu (Eds.) Computer Engineering and Networking, Springer, 2014 (pp. 465-472).
[18] Y. Yao, M.-H. Wan, W. Huang, Robust Low-Rank Discriminant Embedded Regression, Journal of Nanjing University of Aeronautics and Astronautics 53(5)(2021) 692-699.
[19] R. Mokni, M. Elleuch, M. Kherallah, Biometric palmprint identification via efficient texture features fusion, in: Proc. International Joint Conference on Neural Networks, 2016.
[20] Y.-L.-M. Latha, M.-V.-N.-K. Prasad, Intramodal palmprint recognition using texture feature, International Journal of Intelligent Systems Design and Computing 1(1/2)(2017) 168-185.
[21] S. Zhang, H. Wang, W. Huang, C. Zhang, Combining modified LBP and weighted SRC for palmprint recognition, Signal Image & Video Processing 12(6)(2018) 1035-1042.
[22] Q.-L. Sun, J.-X. Zhang, A.-Q. Yang, Q. Zhang, Palmprint recognition with deep convolutional features, in: Proc. of the Chinese Conference on Image and Graphics Technologies, 2017.
[23] S. Zhao, B. Zhang, Deep discriminative representation for generic palmprint recognition, Pattern Recognition 98(2020) 107071.
[24] H.-L. Wang, S.-J. Li, W. Jia, X.-P. Liu, Performance evaluation of convolutional neural network in palmprint recognition, Journal of Image and Graphics 24(8)(2019) 1231-1248.
[25] L.-K. Fei, B. Zhang, Y. Xu, W. Jia, J. Wen, J. Wu, Precision direction and compact surface type representation for 3D palmprint identification, Pattern Recognition 87(2019) 237-247.
[26] K. Balasamy, D. Shamia, Feature extraction-based medical image watermarking using fuzzy-based median filter, IETE Journal of Research 69(1)(2023) 83-91.
[27] L. Salimi, A. Haghighi, A. Fathi, A novel watermarking method based on differential evolutionary algorithm and wavelet transform, Multimedia Tools and Applications 79(17-18)(2020) 11357-11374.
[28] D.-X. Zhong, J.-S. Zh, X.-F. Du, Progress of palmprint recognition: A review, Pattern Recognition and Artificial Intelligence 32(5)(2019) 436-445.
[29] F.-J. Ren, Y.-Q. Li, L.-F. Xu, M. Hu, X.-H. Wang, Face recognition method based on local mean pattern description and double weighted decision fusion for classification, Journal of Image and Graphics 21(5)(2016) 565-573
[30] Y.-Z. Liu, Z.-Q. Jiang, N. Zhao, Three dimensional palmprint recognition based on neighbor ternary pattern and collaborative representation, Journal of Computer Applications 39(6)(2019) 1690-1695.
[31] J. Chaudhari, H. Mewada, A. Patel, K. Mahant, A. Vala, Computationless palm-print verification using wavelet oriented zero-crossing signature, IIUM Engineering Journal 23(1)(2022) 222-232.
[32] Y.-Z. Liu, X.-J. Fan, S. Lin, 3D palmprint recognition based on local orientation binary pattern combined with collaborative representation, Chinese Journal of Liquid Crystals and Displays 37(6)(2022) 726-735.
[33] J.-R. Cui, The research on recognition and fusion methods based on multispectral and 2d/3d palmprint, Harbin: Harbin Institute of Technology 14(2)(2015) 34-41.
[34] B. Yang, W.-B. Mo, J.-L. Yao, 3D palmprint recognition by using local features and deep learning, Journal of Zhejiang University 54(3)(2020) 540-545.